

# CONTACTLESS TORQUE SENSOR

## *Mechatronic Principle and Prototype Development for Automotive Applications*

Manfred Brandl

*Austriamicrosystems AG, Schloss Premstätten, Austria*

Franz Haas, Reinhard Marik

*FH CAMPUS 02, Department of Automation Technology, Körblergasse 126, Graz, Austria*

Keywords: Torque sensor, Inductive principle, Electric steering system, Finite element method.

Abstract: In this paper fundamentals and the prototype development of a new contactless torque sensor are presented. The whole device can be divided into a mechanical and an electromagnetic system. The prototype is designed for the torque range of an electric power assisted steering. The basic idea is the transformation of the shaft twist under torque load into a translational movement of the middle part of the sensor sleeve that is measured by an inductive measuring device. An additional aspect is the low cost manufacturing and assembling of the whole system. The interface electronics ensures high linearity and accuracy and is therefore very suitable for this application. This new sensor concept is very robust and self-compensating for all kinds of relative positioning tolerances ranging from temperature change to external forces.

## 1 INTRODUCTION

The object of this publication is to present a new contactless torque sensor concept based on a highly reliable inductive sensing principle for automotive applications to overcome the drawbacks of present solutions.

Recent automotive fuel saving and power train techniques are requiring highly reliable but low cost torque sensors. One example application is electric power assisted steering system (Graßmann, 2003) to measure input torque. Others are open or closed loop drive train applications such as torque vectoring, power control or power assisted bicycles.

## 2 TORQUE SENSOR PRINCIPLE

Torque measurement on rotating shafts leads to a specific design requirement. The torque information has to be transmitted in a wireless non-contact manner from the rotating shaft to the static readout environment. The technical solution is to pick up the torque information on the rotating shaft and transmit it to a stationary receiver either through electric, magnetic or electromagnetic field.

Today's sensing techniques are:

- Strain gauge or magneto-elastic sensor on shaft surface to measure strain in 45-degree direction versus shaft axis;
- A compliant torsion bar with optical, resistive, inductive or magnetic (Angleviel, 2005) measurement of the relative angle between both ends. This principle is used in modern electromechanical steering systems (Heißing, 2008) and fulfils the requirements of safety and reliability.

At present torque sensors are mostly used in industrial drive train applications, in robotics and in bench test measurement equipment.

For this new concept the system can be divided into two domains:

- Mechanical domain;
- Electromagnetic domain.

### 2.1 Mechanical Domain

The twist of a steel shaft under load is transformed to an axial displacement (Jacobsen, 1944). This effect and the core part of the torque sensor are shown in Figure 1. The applied torque causes a shaft

twist that is induced into a specially designed sleeve. This part, for instance made of aluminium, is perfectly attached to the shaft at two cylindrical faces with a constant distance. The connections of the middle part to the outside parts represent thin rods that translate the twist into a translational movement ( $\Delta x$ ) along the shaft rotation axis.

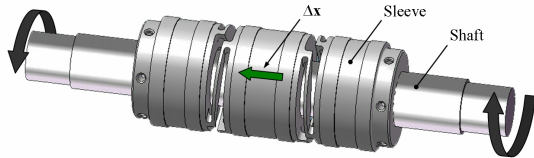


Figure 1: Sleeve with the fixation parts, middle part and connection rods.

Possible manufacturing processes are chipping technologies (turning and milling), powder injection moulding or welded composite from punched parts depending on the production volume.

## 2.2 Electromagnetic Domain

Two fixed ferromagnetic sleeves, one displaceable centre sleeve and the two axial air gaps as part of the rotor are shown in Figure 2.

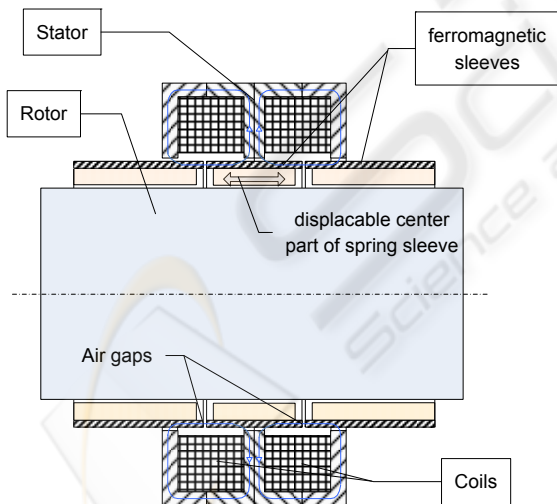


Figure 2: Electro magnetic circuit formed by sensor rotor and sensor stator.

The rotor forms a differential inductive half bridge circuit (see Figure 3) with two fixed coils and its respective ferromagnetic field concentrators as a stator.

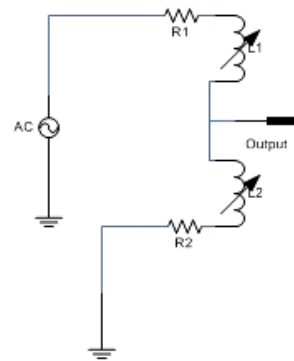


Figure 3: Sensor inductances and its parasitic resistances connected in series to form a half bridge.

The stationary coils and their ferromagnetic housings are placed concentric to the shaft in the middle of the rotor with the two air gaps. When torque is applied, one air gap increases and the other one gets smaller by the same amount. The two coils are connected in series and excited by a common electrical signal. The reluctance ratio determines the output voltage of the inductive half bridge. The magnetic circuit is designed in such a way that a significant portion of the total reluctance is determined by the axial air gaps between the rotor sleeves. Any differential change of air gap due to applied torque leads to a non-balanced bridge and an output signal linear with displacement in case of small deflections.

Because of the symmetric arrangement of the magnetic ring elements all air gap changes due to shaft bending, shaft expansion or shaft compression won't lead to an output signal. Nor will concentricity errors of the rotor influence the output signal. Even axial simultaneous displacement of the entire rotor like a bearing play will not lead to reluctance difference in the first instance. Most important is that also shaft rotation doesn't affect the balance of the electromagnetic circuit, either.

An important point is the matching of both air gaps at zero torque. Any offset would lead to unbalanced bridge and therefore to a temperature drift of the sensor zero point. Also, non equal air gap size over the circumference would lead to 2<sup>nd</sup> order effects causing small output changes with angular rotor position. Therefore it is proposed that the ferromagnetic sleeves are separated exactly after bonding by laser cutting.

As a conclusion it is obvious that this sensor concept is very robust and self-compensating for all kinds of relative positioning tolerances ranging from temperature change, bearing play and forces applied to the stator or rotor shaft.

### 3 SENSOR OPTIMIZATION

This chapter describes the basic kinematical principle and the FEM-optimization of the torque sensor geometry (Marik, 2008). Optimization criteria are the translational movement  $\Delta x$ , but also the costs for manufacturing and assembling.

#### 3.1 Kinematical Principle

Basically the sensibility of the torque sensor depends on the translation  $\Delta x$  which is directly linked to the current torsion angle. The formal correlation of the torsion angle ( $\varphi$ ), the torque ( $M_x$ ), the length of the casing ( $l$ ), the modulus of rigidity ( $G$ ) and the polar area moment ( $I_p$ ) is shown in equation (1).

$$\varphi = \frac{M_x * l}{G * I_p} * \frac{180}{\pi} \quad (1)$$

In most cases the shaft diameter, the external torque, the material of the shaft and the possible casing length are given values and cannot be changed. Concerning the example of an 18mm diameter steering shaft, a torsion angle  $\varphi$  from 0.05 to 0.06 degrees leads to a twist movement on the shaft surface of 0.02mm. According to that point the only way to achieve a maximum  $\Delta x$  is to optimize the design of the mechanical sleeve.

The simplified function model of the sleeve is a two rod system with three revolute joints. Figure 4 shows the situation on a flat surface to demonstrate the geometrical relationships more easily.

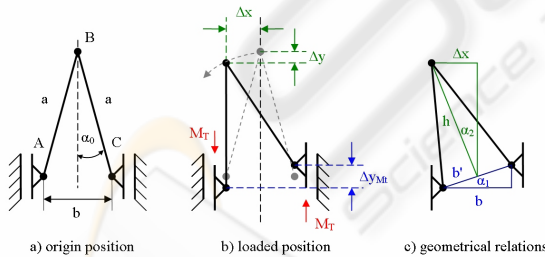


Figure 4: Simplified function model of the sleeve on a flat surface.

Two rods with the length ( $a$ ) are connected to each other at joint (B) and to the surrounding at joints (A) and (C) (see Figure 4a). The connection points A and B are only moveable in the  $y$ -direction but fixed in the  $x$ -direction. When the system gets loaded due to a torque the points A and C move contrarily along the  $y$ -direction ( $\Delta y_{Mt}$ ) and hence the

joint B moves from its origin position along a circular path with the radius ( $a$ ) (see Figure 4b).

The geometrical relations in  $x$ -direction are shown in Figure 4c and can be described in equation (2).

$$\Delta x = \sqrt{a^2 - \frac{b^2 + \Delta y_{Mt}^2}{4}} * \sin(\tan^{-1}(\frac{\Delta y_{Mt}}{b})) \quad (2)$$

From equation (2) it is obvious that the achieved  $\Delta x$  is linear depending on the length ( $a$ ) and nonlinear to the geometric relation of  $\Delta y_{Mt}$  and the width ( $b$ ), the tilt angle of the system. But when the two rod system gets wrapped around a cylindrical surface the interacting rod length will be scaled down by the influence of the cylinder radius  $R$  as shown in Figure 5.

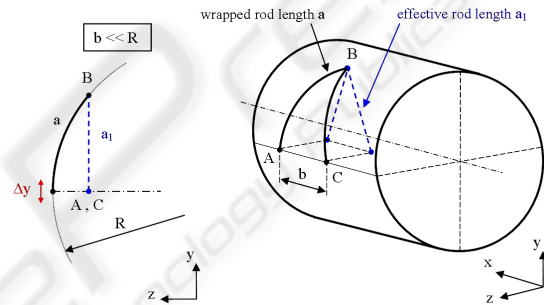


Figure 5: Function model on a cylindrical surface.

Consequently to that effect the linear impact of length ( $a$ ) gets nonlinear according equation (3) under the precondition that the distance ( $b$ ) is very short in relation to the radius ( $R$ ) ( $b \ll R$ ).

$$a_1 = R * \sin(\frac{a}{R}) \quad (3)$$

It is obvious that ( $a_1$ ) has its maximum value when ( $a$ ) is the quarter of the cylinder circumference, which is an important fact for the geometry of the rotor rod elements.

#### 3.2 FEM-Studies

Based on the kinematical principle the final CAD-design has to be defined. The optimized shape of the measuring sleeve (see Figure 1) is characterized by a maximum  $\Delta x$  and a light structure with high stiffness. Simulation helps to accelerate the development process and to increase the quality of the first prototype (Seiffert, 2008). The stresses in critical regions near the revolute joint positions must be under the fatigue limit of the chosen aluminium alloy. The prototype sleeve is to be made as a turning-milling part. Therefore the minimum cutting

tool diameter and the attainable lowness of the inner undercuts also have to be considered.

Figure 6 shows the displacement ( $dx$ ) in the direction of the shaft axis. It is the result of a static FEM analysis with the external torque at one side and the fixation at the other side as model constraints.

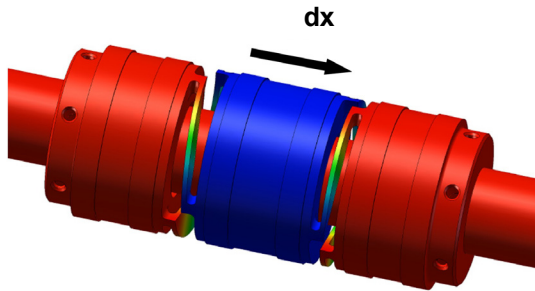


Figure 6: FEM result of displacement  $dx$ .

A satisfying compliance between measurement results and simulation has been found (see Figure 7). The measurement setup is illustrated in Figure 8.

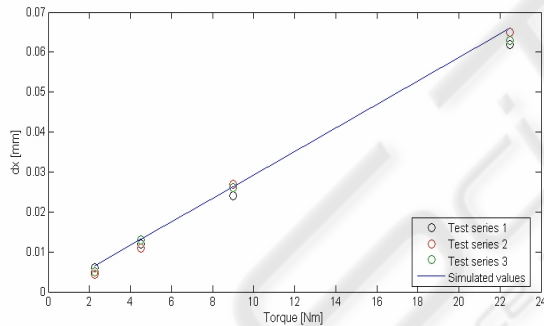


Figure 7: Comparison between measuring and simulation.

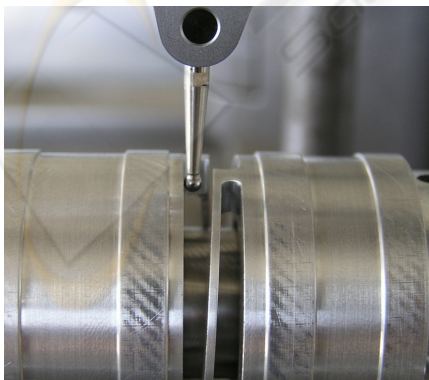


Figure 8: Measurement setup.

In addition theoretical considerations can be proved by reducing the dimensions of the joint connections. Figure 9 shows the differences between the results of the basic kinematic model and the FEM simulations by varying rod lengths (a). Figure 10 gives an overview about changes of ( $dx$ ) with different values (b).

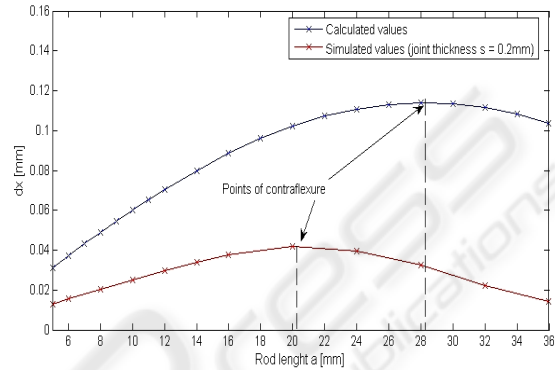


Figure 9: Displacement values with various rod lengths.

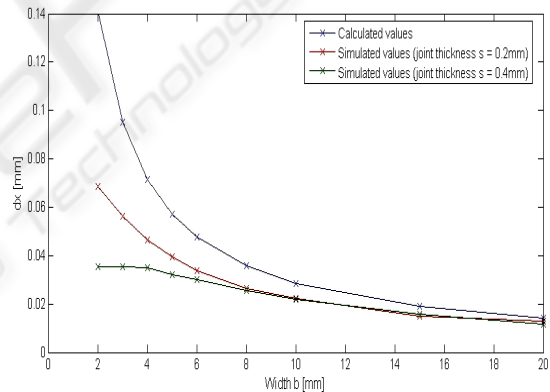


Figure 10: Displacement values with various values  $b$ .

## 4 INTERFACE ELECTRONICS

The inductive half bridge is supplemented by a resistive voltage divider to form a Maxwell bridge. Its output signal is amplified and converted to digital output with high precision by an integrated data acquisition circuit. The block diagram in Figure 11 shows the setup of the interface electronics.

Today's semiconductor circuit design techniques enable us to conquer new domains in precision and ultra low drift signal conditioning unreachable just a few years ago.

For this torque sensor an integrated data

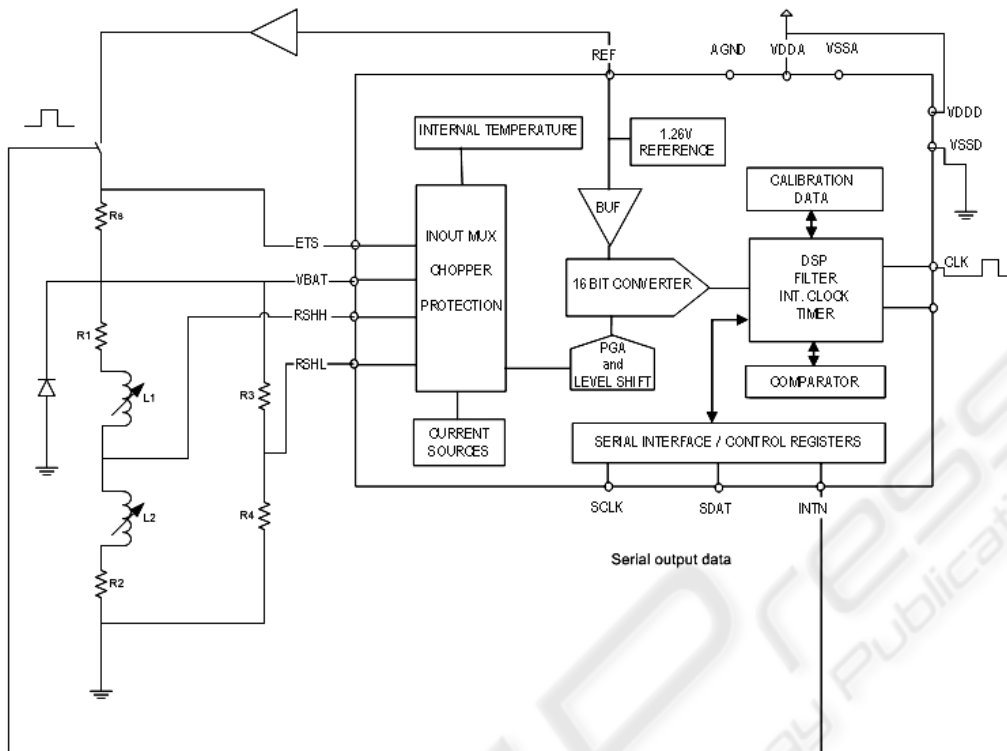


Figure 11: Block diagram of sensor interface electronics.

acquisition device was used which was specifically designed to convert very small voltages to digital domain with very high precision.

This data acquisition device offers two multiplexed fully differential input channels, a programmable gain amplifier, a 16 bit analog to digital converter and a serial interface for device configuration and result read-out.

Special auto zero offset architecture offers virtually zero offset below  $0.5\mu\text{V}$  and very low noise. The analog to digital converter is of Sigma-Delta type, an architecture which offers high linearity without any missing codes.

The device has an integrated trim-able precision reference and a temperature compensation for the entire measurement path. The integrated circuit also offers a measurement-ready signal which is used to excite the transducer bridge with a pulsed DC voltage in conjunction with a diode which is to discharge the energy stored in the coils after each applied pulse.

The second channel can be used to measure the bridge current to compensate the temperature coefficient of the copper coil which would otherwise lead to a scaling error. If the digital representation of the bridge voltage is multiplied by compensation factor proportional to the bridge current in an

external micro controller, the final output signal can be made independent from temperature. In that case the coil wires are acting as a temperature sensor.

The development of the electronic system was carried out at the Department of Automation Technology at FH *CAMPUS* 02 in collaboration with austriamicrosystems Corporation applying the newest chip generation (Pauritsch, 2008).

## 5 TEST SYSTEM

Based on the presented solution a test system has been developed that demonstrates a steering (see Figure 12). For that purpose the demonstrator consists of a steering shaft with torque sensor and rotary encoders, two bearings and a steering wheel.

### 5.1 Torque Sensor

The torque sensor is placed in the middle of the bearing houses. The sensor sleeve is pinned on the 18 mm diameter shaft to induce the shaft twist into the sleeve. The stator part consists of a casing with two coils and four ferromagnetic concentrators forming two inductances in the range of 10mH with

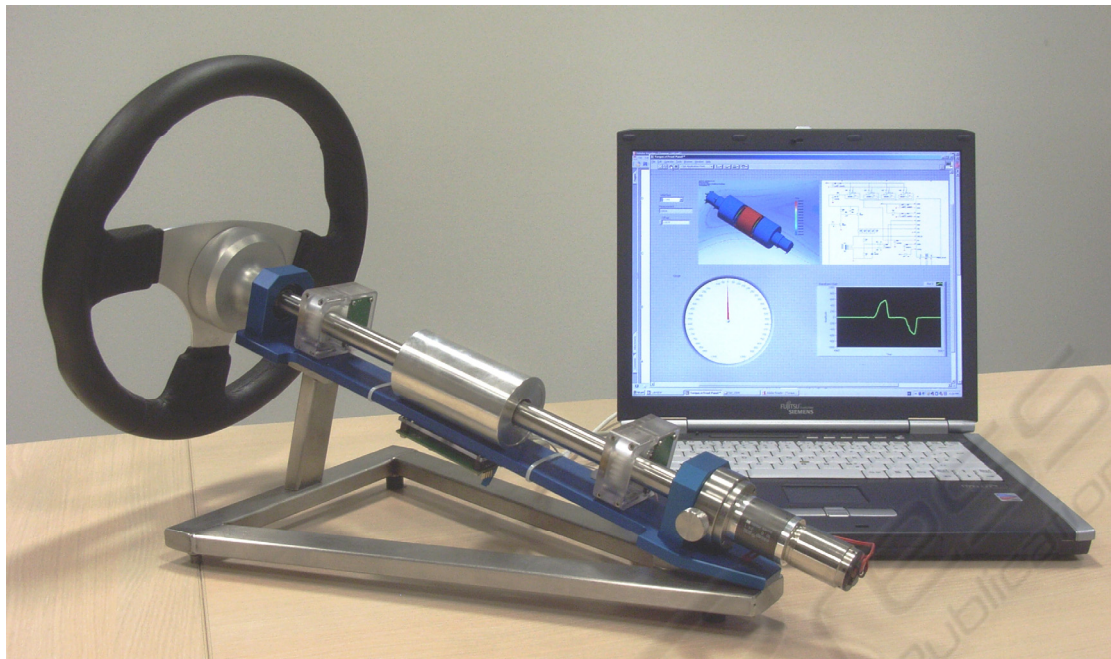


Figure 12: Steering demo system with one torque sensor, two rotary encoders and Graphical- User-Interface (GUI) for torque measurement.

400 windings of 0,15mm copper wire. The entire coil arrangement is fixed by two screwed covers.

The stator has to be aligned to the axis of the shaft carefully.

The coil wires are led through small holes and connected with the sensor interface. The PCB is mounted on the base plate of the demonstrator. The steering torque can be simulated by a DC-motor or by a special brake with a fixation screw.

## 5.2 Rotary Encoder

In addition to the torque measurement the steering angle is also measured at two positions by using Hall-sensors.

The rotary encoder (Czichos, 2008) consists of a small magnet disc with north/south pole, which rotates at a very short distance to the Hall-sensor-chip. This disc is directly mounted on a small gearwheel. The according gear consists of the pinion gear with the magnet and a gearwheel that is fixed on the steering shaft. The casing of the rotary encoder is separated into two parts for easy assembling and also includes the sensor PCB.

## 5.3 User Interface

The user interface software is programmed with “Labview” and enables various types of graphical

representation of the measurement results.

## 5.4 Linearity Measurement

The characteristic of the new sensor is the result of measurements within a specified torque range of  $\pm 5\text{Nm}$ . Figure 13 shows the sensor output signal which is virtually linear with torque without any hysteresis.

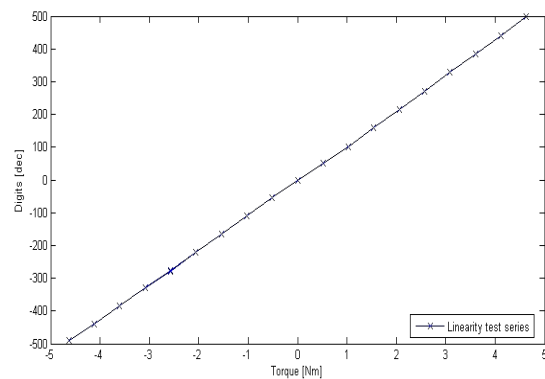


Figure 13: Torque sensor characteristic without any hysteresis.

## 6 CONCLUSIONS

A contactless torque sensor for accurate and reliable low frequency torque measurement on a rigid steering shaft has been introduced. The principle is in our opinion well suited to develop a low cost sensor product with adequate values of repeatability, accuracy and reliability. The cost and quality targets can be achieved, if manufacturing techniques like laser cutting and laser welding will be utilized.

The entire mechatronic solution is based on well known design elements which do not lead to long term drifts of zero point and output scale. There is virtually no hysteresis in output signal as proven by the demonstrator design.

It has to be pointed out that the design of a final sensor product has to consider sufficient spring stiffness in axial direction as well as low mass for the displaceable centre sleeve spring/mass system to ensure insignificant displacement when the sensor is exposed to low frequency or constant acceleration. It has to be ensured that its first mode resonance frequency is higher than the frequency band of interest.

Our contribution represents a preparatory study for any subsequent mechatronic product development.

Due to the number of involved technical disciplines like mechanical-, electromagnetic-, electronic-, manufacturing- and safety engineering it is recommended to continue the research work as an academic project in conjunction with other universities and industrial partners.

We are confident that as a result of such R&D-activities a new type of mechatronic torque sensor device with unmatched performance versus cost ratio can be placed on the market for many applications.

## REFERENCES

- Angleviel, D., Frachon, D., and Masson, G., 2006. *Development of a Contactless Hall effect torque sensor for Electric Power Steering*. MMT S.A.
- Czichos, H., 2008. *Mechatronik*. P 217. Vieweg+Teubner Verlag. Wiesbaden.
- Graßmann, O., Henrichfreise, H., Niessen H., and Hammel K., 2003. *Variable Lenkunterstützung für eine elektromechanische Servolenkung*. 23. Tagung "Elektronik im Kfz". Stuttgart.
- Heißing, D., Ersoy M., 2008. *Fahrwerkhandbuch*. pp 209-215. Vieweg+Teubner Verlag. Wiesbaden.
- Jacobsen, A.M., 1944. *Electrical Dynamometer*. US Patent Application Serial No. 561,467. Los Angeles.

- Marik, R., 2008. *Konturoptimierung einer Messnabe*. Bachelor Thesis. FH CAMPUS 02. Graz.
- Pauritsch, M., 2008. *Product documentation of the sensor interface*. Graz..
- Seiffert, U., Rainer G., 2008. *Virtuelle Produktentstehung für Fahrzeug und Antrieb im Kfz*. pp 7-29. Vieweg+Teubner Verlag. Wiesbaden.